A unified approach to realize universal quantum gates in a coupled two-qubit system with fixed always-on coupling

Zhongyuan Zhou[1,2], Shih-I Chu[1], and Siyuan Han[2]
[1]*Department of Chemistry, University of Kansas, Lawrence, KS 66045*
[2]*Department of Physics and Astronomy, University of Kansas, Lawrence, KS 66045*
(Received: June 29, 2005)

Abstract

We demonstrate that in a coupled two-qubit system any single-qubit gate can be decomposed into two *conditional* two-qubit gates and that any *conditional* two-qubit gate can be implemented by a manipulation analogous to that used for a controlled two-qubit gate. Based on this we present a unified approach to implement universal single-qubit and two-qubit gates in a coupled two-qubit system with fixed always-on coupling. This approach requires neither supplementary circuit or additional physical qubits to control the coupling nor extra hardware to adjust the energy level structure. The feasibility of this approach is demonstrated by numerical simulation of single-qubit gates and creation of two-qubit Bell states in rf-driven inductively coupled two SQUID flux qubits with realistic device parameters and constant always-on coupling.

PACS numbers: 03.67.Lx, 85.25.Dq, 03.67.Mn

During the past decade, a variety of physical qubits have been explored for possible implementation of quantum gates. Of those solid-state qubits based on superconducting devices have attracted much attention because of their advantages of large-scale integration and easy connection to conventional electronic circuits [1, 2, 3, 4, 5, 6, 7, 8, 9, 10, 11, 12, 13, 14, 15]. Superconducting single-qubit gates [4, 5, 6, 7, 8, 9, 10, 11] and two-qubit gates [12, 13, 14, 15] have been demonstrated recently.

However, building a practical quantum computer requires to operate a large number of multi-qubit gates simultaneously in a coupled multi-qubit system. It has been demonstrated that any type of multi-qubit gate can be decomposed into a set of universal single-qubit gates and a two-qubit gate, such as the controlled-NOT (CNOT) gate [16, 17]. Thus it is imperative to implement the universal single-qubit and two-qubit gates in a multi-qubit system with the minimum resource and maximum efficiency [18].

Implementing universal single-qubit gates and two-qubit gates in coupled multi-qubit systems can be achieved by turning off and on the coupling between qubits [18, 19, 20]. In these schemes, supplementary circuits were required to control inter-qubit coupling. However, rapid switching of the coupling results in two serious problems. The first one is gate errors caused by population propagation between qubits. Because the computational states of the single-qubit gates are not a subset of the eigenstates of the two-qubit gates the populations of the computational states propagate from one qubit to another when the coupling is changed, resulting in additional gate errors. The second one is additional decoherence introduced by the supplementary circuits [21, 22]. This is one of the biggest obstacles for quantum computing with solid-state qubits, particularly in coupled multi-qubit systems [2]. In addition, the use of supplementary circuits also significantly increase the complexity of fabrication and manipulation of the coupled qubits.

To circumvent these problems, a couple of alternative schemes, such as those with untunable coupling [21] and always-on interaction [23], have been proposed. In the first scheme, each logic qubit is encoded by extra physical qubits and coupling between the encoded qubits is constant but can be turned off and on effectively by putting the qubits in and driving them out of the interaction free subspace. In the second scheme, the coupling is always on but the transition energies of the qubits are tuned individually or collectively. These schemes can overcome the problem of undesired population propagation but still suffer from those caused by the supplementary circuits needed to move the encoded qubits and tune the transition energies. Moreover, the use of encoded qubits also requires a significant number of additional physical qubits.

In this Letter, we present a unified approach to implement universal single-qubit and two-qubit gates in a coupled two-qubit system with fixed always-on coupling. In this approach, each single-qubit gate is realized via two *conditional* two-qubit gates and each *conditional* two-qubit gate is implemented with a manipulation analogous to that used for a controlled two-qubit gate (e.g., CNOT) in the same subspace of the coupled two-qubit system without additional circuits or physical qubits. Since the computational states of the single-qubit gates are a subset of those of the two-qubit gates the gate errors due to population propagation are completely eliminated. The effectiveness of the approach is demonstrated by numerically simulating the single-qubit gates and creating the Bell states in a unit of inductively coupled two superconducting quantum interference device (SQUID) flux qubits with realistic device parameters and constant always on coupling.

Consider a basic unit consisting of two coupled qubits which we call a control qubit ($\mathcal{C}q$) and a target qubit ($\mathcal{T}q$) for convenience. An eigenstate of the coupled qubits is

denoted by $|n) = |ij\rangle$, which can be well approximated by the product of an eigenstate of $\mathcal{C}q$, $|i\rangle$, and that of $\mathcal{T}q$, $|j\rangle$, $|n) \equiv |ij\rangle = |i\rangle |j\rangle$, for weak inter-qubit coupling. The computational states of the coupled qubits are $|1) = |00\rangle$, $|2) = |01\rangle$, $|3) = |10\rangle$, and $|4) = |11\rangle$, which correspond to the eigenstates for i, j = 0, 1 and n = 1, 2, 3, 4, respectively. In general, the result of an operation on $\mathcal{C}q$ depends on the state of $\mathcal{T}q$ since $\mathcal{C}q$ is coupled to and hence influenced by $\mathcal{T}q$. Suppose U is a unitary operator acting on a single qubit in the four-dimensional (4D) Hilbert space spanned by $|n)$. In order to perform U on $\mathcal{C}q$ one wants the state of $\mathcal{C}q$ evolves according to U independent of the state of $\mathcal{T}q$ which is left unchanged. This operation is denoted by $U^{(2)} = U_C^{(1)} \otimes I_T^{(1)}$, where, the 4×4 unitary matrix $U^{(2)}$ and the 2×2 unitary matrix $U_C^{(1)}$ are the representations of U in the Hilbert space of the coupled qubits and in the subspace of $\mathcal{C}q$ while the 2×2 unitary matrix $I_T^{(1)}$ is the representation of the identity operation in the subspace of $\mathcal{T}q$. If the matrix elements of $U_C^{(1)}$ are u_{ij} $(i, j = 1, 2)$ the operation can be decomposed into two operations as

$$U^{(2)} = \begin{pmatrix} 1 & 0 & 0 & 0 \\ 0 & u_{11} & 0 & u_{12} \\ 0 & 0 & 1 & 0 \\ 0 & u_{21} & 0 & u_{22} \end{pmatrix} \begin{pmatrix} u_{11} & 0 & u_{12} & 0 \\ 0 & 1 & 0 & 0 \\ u_{21} & 0 & u_{22} & 0 \\ 0 & 0 & 0 & 1 \end{pmatrix} = U_1^{(2)} U_0^{(2)}, \tag{1}$$

where, the 4×4 unitary matrices $U_0^{(2)}$ and $U_1^{(2)}$ are also in the 4D Hilbert space of the coupled qubits. Since $U_0^{(2)}$ only involves the states $|00\rangle$ and $|10\rangle$ and $U_1^{(2)}$ only involves $|01\rangle$ and $|11\rangle$ they represent operations on $\mathcal{C}q$ when $\mathcal{T}q$ is in the state $|0\rangle$ and $|1\rangle$, respectively. If the state of $\mathcal{T}q$ is $|0\rangle$ ($|1\rangle$), $U_0^{(2)}$ ($U_1^{(2)}$) implements the desired operation U while $U_1^{(2)}$ ($U_0^{(2)}$) does nothing. Thus $U_0^{(2)}$ and $U_1^{(2)}$ represent two conditional two-qubit gates of the coupled qubits. Eq.(1) shows that for the coupled qubits *any single-qubit gate can be realized via two conditional two-qubit gates*. This property is universal and is shown schematically in Fig. 1, where the single-qubit operation $U^{(2)}$ and its equivalent operation via two conditional two-qubit gates $U_0^{(2)}$ and $U_1^{(2)}$ are illustrated. The conditional gates are denoted by the open and closed circles for the state of $\mathcal{T}q$ being $|0\rangle$ and $|1\rangle$, respectively [16].

The most obvious advantage of implementing single-qubit gates this way is that the conditional two-qubit gates can be realized using essentially the same set of operations used for controlled two-qubit gates. To show this, let us consider a rf-driven coupled two-qubit system with sufficiently different energy-level spacings ΔE_{13}, ΔE_{24}, ΔE_{12}, and ΔE_{34}, where $\Delta E_{nn'}$ is the level spacing between the states $|n)$ and $|n')$. To implement, for example, a single-qubit NOT gate, we apply two π pulses to the $\mathcal{C}q$: the first one is resonant with ΔE_{13} and the second with ΔE_{24}. Because both pulses are largely detuned from ΔE_{12} and ΔE_{34}, they do not induce unintended population transfer when the fields are sufficiently weak. If the state of $\mathcal{T}q$ is $|0\rangle$ ($|1\rangle$), the first (second) pulse accomplishes the desired transformation. Therefore, when the two microwave pulses are applied to $\mathcal{C}q$, either sequentially or simultaneously, the NOT gate is accomplished and the gate time is essentially the same as that of a stand-alone $\mathcal{C}q$ if the both pulses are applied simultaneously.

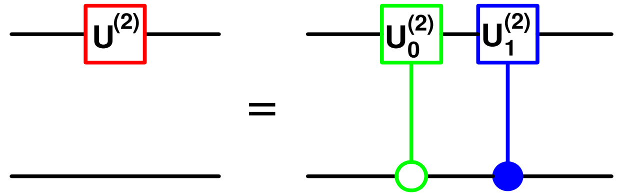

FIG. 1: Single-qubit gate $U^{(2)}$ and its equivalent operation by two conditional two-qubit gates $U_0^{(2)}$ and $U_1^{(2)}$ in a coupled two-qubit system.

To implement a two-qubit gate such as CNOT in coupled qubits, we apply a π pulse resonant with ΔE_{34} to $\mathcal{T}q$ [24]. In this case, the state of $\mathcal{T}q$ flips if and only if the state of $\mathcal{C}q$ is $|1\rangle$. Since the energy level structure for the conditional two-qubit gates and the CNOT gate could be the same the universal single-qubit gates and CNOT gate can be implemented in the same fashion without adjusting inter-qubit coupling as long as $\mathcal{C}q$ and $\mathcal{T}q$ can be addressed individually by microwave pulses, which is rather straightforward to realize with solid-state qubits in general and with rf SQUID flux qubits in particular.

For concreteness, we demonstrate how to realize the single-qubit and two-qubit gates in rf-driven two SQUID flux qubits with constant always-on coupling. The coupled flux qubits comprise two SQUIDs coupled inductively through their mutual inductance M. Each SQUID consists of a superconducting loop of inductance L interrupted by a Josephson tunnel junction characterized by its critical current I_c and shunt capacitance C [25]. A flux-biased SQUID with total magnetic flux Φ enclosed in the loop is analogous to a "flux" particle of mass $m = C\Phi_0^2$ moving in a one-dimensional potential, where $\Phi_0 = h/2e$ is the flux quantum. For simplicity, we assume that the two SQUIDs are identical. In this case, $C_i = C$, $L_i = L$, and $I_{ci} = I_c$ for $i = 1, 2$. The Hamiltonian of the coupled qubits is [24, 26] $H(x_1, x_2) = H_0(x_1) + H_0(x_2) + H_{12}(x_1, x_2)$, where $H_0(x_i)$ is Hamiltonian of the ith single qubit given by $H_0(x_i) = p_i^2/2m + m\omega_{LC}^2 (x_i - x_{ei})^2/2 - E_J \cos(2\pi x_i)$ and H_{12} is the interaction between the SQUIDs given by $H_{12} = m\omega_{LC}^2 \kappa (x_1 - x_{e1})(x_2 - x_{e2})/2$. Here, $x_i = \Phi_i/\Phi_0$ is the canonical coordinate of the ith "flux" particle and $p_i = -i\hbar\partial/\partial x_i$ is the canonical momentum conjugate to x_i, $x_{ei} = \Phi_{ei}/\Phi_0$ is the normalized external

flux bias of the ith qubit, $E_J = m\omega_{LC}^2 \beta_L / 4\pi^2$ is the Josephson coupling energy, $\beta_L = 2\pi L I_c / \Phi_0$ is the potential shape parameter, $\omega_{LC} = 1/\sqrt{LC}$ is the characteristic frequency of the SQUID, and $\kappa = 2M/L$ is the coupling strength. The coupled SQUID qubits are a multi-level system. The eigenenergies E_n and eigenstates $|n)$ are obtained by numerically solving the eigenvalue equation of $H(x_1, x_2)$ using the two-dimensional Fourier-grid Hamiltonian method [27]. When x_{e1} and $x_{e2} \sim 0.5$ the coupled SQUID qubits have four wells in the potential energy surface [24]. The four computational states are chosen to be the lowest eigenstate of each well.

To realize single-qubit and two-qubit gates in the coupled SQUID qubits, we apply microwave pulses x_C and x_T to $\mathcal{C}q$ and $\mathcal{T}q$, respectively. The interaction of the coupled qubits and pulses is $V(x_1, x_2, t) = d_1 (x_1 - x_{e1}) + d_2 (x_2 - x_{e2}) + d_{12}$ with $d_1 = m\omega_{LC}^2 (x_C + \kappa x_T/2)$, $d_2 = m\omega_{LC}^2 (x_T + \kappa x_C/2)$, and $d_{12} = m\omega_{LC}^2 \left(x_C^2 + x_T^2 + \kappa x_C x_T\right)/2$. The time-dependent wave functions of the coupled SQUID qubits, $\psi(x_1, x_2, t)$, are governed by the time-dependent Schrödinger equation $i\hbar \partial\psi/\partial t = [H(x_1, x_2) + V(x_1, x_2, t)]\,\psi$. To solve this equation we expand ψ in terms of the first 20 eigenstates of the coupled qubits: $\psi = \sum_n c_n(t)\,|n)$. The expansion coefficients $c_n(\tau)$ are calculated by numerically solving the matrix equation $i\partial c_n(\tau)/\partial\tau = \sum_{n'} H_{nn'}^R(\tau)\, c_{n'}(\tau)$ using the split-operator method [28], where $\tau = \omega_{LC} t$ is the dimensionless time and $H_{nn'}^R = [E_n \delta_{nn'} + (n|V|n')]/\hbar\omega_{LC}$ is the reduced Hamiltonian matrix element. The probability of being in the state $|n)$ is thus $|c_n(\tau)|^2$. For single-qubit gates two resonant pulses, $x_{C1} = x_{C10}\cos(\omega_{C1} t)$ with $\omega_{C1} = \Delta E_{13}/\hbar$ and $x_{C2} = x_{C20}\cos(\omega_{C2} t)$ with $\omega_{C2} = \Delta E_{24}/\hbar$, are applied simultaneously to the $\mathcal{C}q$ so that $x_C = x_{C1} + x_{C2}$. For controlled two-qubit gates such as the CNOT gate one resonant pulse $x_T = x_{T0}\cos(\omega_T t)$ with $\omega_T = \Delta E_{34}/\hbar$ is applied to the $\mathcal{T}q$. To minimize the possible intrinsic gate errors caused by leakage to unintended states, we select the parameters of the coupled SQUID qubits using the independent transition approach [29]. For SQUIDs with $L = 100$ pH, $C = 40$ fF, and $\beta_L = 1.2$ one set of the better working parameters is $x_{e1} = 0.499$, $x_{e2} = 0.4998$, and $\kappa = 5 \times 10^{-4}$, which will be used in the calculation.

Most of the single-qubit gates, such as the NOT gate and Hadamard gate, can be described by rotations of the state vector on the Bloch sphere [16]. Thus we demonstrate how to realize an arbitrary single-qubit rotation of an angle θ about an axis perpendicular to the z axis, $R^{(2)}(\theta)$, in the coupled SQUID qubits. Based on Eq.(1), the rotation $R^{(2)}(\theta)$ on $\mathcal{C}q$ is accomplished via two conditional two-qubit rotations $R_0^{(2)}(\theta)$ and $R_1^{(2)}(\theta)$ as shown in FIG. 2(a). They are realized by applying two microwave pulses x_{C1} and x_{C2} to $\mathcal{C}q$ simultaneously. The amplitudes and frequencies of x_{C1} and x_{C2} are $x_{C10} = 5 \times 10^{-5}$, $\omega_{C1} = 0.239\omega_{LC} = 2\pi \times 19.0$ GHz,

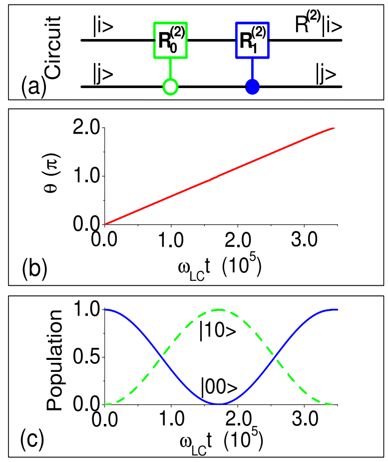

FIG. 2: Arbitrary single-qubit rotation about an axis perpendicular to z axis in the coupled SQUID flux qubits. (a) Quantum circuit: the state $|ij\rangle$ evolves to the state $R^{(2)}(\theta)\,|ij\rangle = \left[R^{(2)}(\theta)\,|i\rangle\right]|j\rangle$ after the two conditional two-qubit rotations. (b) The rotation angle θ vs. pulse width. (c) Populations of the states $|00\rangle$ and $|10\rangle$ vs. pulse width.

$x_{C20} = 5.14 \times 10^{-5}$, and $\omega_{C2} = 0.259\omega_{LC} = 2\pi \times 20.6$ GHz. In Fig. 2 (b) and (c), we plot the rotation angle θ and the populations of the states $|00\rangle$ and $|10\rangle$ (populations of the other states remain essentially at zero) as a function of pulse width when the initial state of the coupled qubits is $|00\rangle$. It is shown in Fig. 2 (b) that the rotation angle θ is essentially a linear function of pulse width. This indicates that the state of $\mathcal{C}q$ undergoes Rabi oscillations for which the phase angle $\Omega\tau$ is a linear function of pulse width, where Ω is the Rabi frequency. It is also shown in Fig. 2 (c) that from the initial state $|00\rangle$ the coupled qubits evolve into the state $(|00\rangle + |10\rangle)/\sqrt{2}$ after the $\pi/2$ pulses and into the state $|10\rangle$ after the π pulses. We have also computed the rotation angles and populations for the coupled qubits with the initial states $|01\rangle$, $|10\rangle$, and $|11\rangle$ using the same pulse sequence. In each case, the state is transformed from $|ij\rangle$ to $R^{(2)}(\theta)\,|ij\rangle = \left[R^{(2)}(\theta)\,|i\rangle\right]|j\rangle$ for $i, j = 0, 1$ with $\theta = \Omega\tau$ as expected.

Entanglement is one of the most profound characteristics of quantum systems which plays a crucial role in quantum information processing and communication [16]. The maximally entangled two-qubit states are referred to as the Bell states. To create the Bell states from a state $|ij\rangle$, a Hadamard gate on $\mathcal{C}q$, $H^{(2)}$, which is decomposed into two conditional two-qubit Hadamard gates $H_0^{(2)}$ and $H_1^{(2)}$, and a CNOT gate are commonly used [see FIG. 3(a)]. The two conditional two-qubit Hadamard gates are implemented by applying two $\pi/2$ pulses x_{C1} and x_{C2} to $\mathcal{C}q$ and the following CNOT gate is implemented by applying a π pulse x_T to $\mathcal{T}q$, as shown

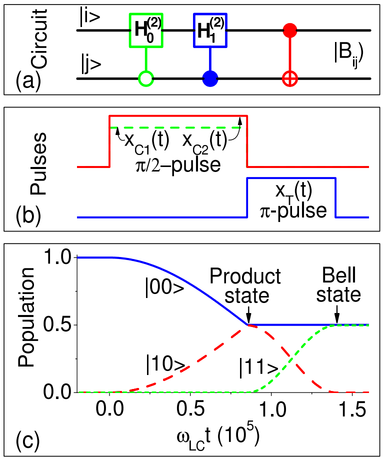

FIG. 3: Creation of the Bell states in the coupled SQUID flux qubits. (a) Quantum circuit: the state $|ij\rangle$ evolves into an entangled state $|B_{ij}\rangle$ after two conditional two-qubit Hadamard gates and one CNOT gate. (b) Microwave pulses: two $\pi/2$ pulses x_{C1} and x_{C2} are applied to the $\mathcal{C}q$ first and then a π pulse x_T is applied to the $\mathcal{T}q$. (c) Population evolution: the coupled qubits evolve into a product state $\left(|00\rangle + |10\rangle\right)/\sqrt{2}$ from the initial state $|00\rangle$ after the first two $\pi/2$ pulses and then into a Bell state $\left(|00\rangle + |11\rangle\right)/\sqrt{2}$ from the product state after the second π pulse.

in FIG. 3(b). The amplitudes and frequencies of x_{C1} and x_{C2} are the same as those used in FIG. 2 and those of x_T are $x_{T0} = 5 \times 10^{-5}$ and $\omega_T = 0.0592\omega_{LC} = 2\pi \times 4.7$ GHz. In FIG. 3(c), we plot the population evolution of the computational states when the initial state is $|00\rangle$. It is shown clearly that the coupled qubits evolve first into a product state $\left(|00\rangle + |10\rangle\right)/\sqrt{2}$ from the initial state $|00\rangle$ after the $\pi/2$ pulses and then into a Bell state $\left(|00\rangle + |11\rangle\right)/\sqrt{2}$ after the subsequent π pulse. We have also calculated the population evolution for the coupled qubits being initially in $|01\rangle$, $|10\rangle$, and $|11\rangle$, respectively. The final state in each case is also one of the expected Bell states.

In summary, we showed that in a coupled two-qubit system *any single-qubit gate can be realized via two conditional two-qubit gates* and that *any conditional two-qubit gate can be implemented with a manipulation analogous to that used for a controlled two-qubit gate*. Based on this universal property of single-qubit gates we present a general approach to implement the universal single-qubit and two-qubit gates in the same coupled two-qubit system with fixed always-on coupling. This approach is demonstrated by using a unit of two SQUID flux qubits with realistic device parameters and constant always-on coupling. Compared to other methods our approach has the following characteristics and advantages: (1) The approach is universal as long as each qubit can be locally addressed; (2) No additional decoherence from the hardware added to control inter-qubit coupling; (3) Gate error induced by the population propagation from one qubit to another is completely eliminated; (4) The architecture for both hardware (circuits) and software (pulse sequence) is much simplified. This approach can be readily extended to multi-qubit systems and other types of solid-state qubit systems in which each qubit can be individually addressed. Therefore, it is very promising for realizing universal gates with minimum resource and complexity and maximum efficiency.

This work is supported in part by the NSF (DMR-0325551) and by AFOSR, NSA, and ARDA through DURINT grant (F49620-01-1-0439).

[1] A. J. Leggett, Science **296**, 861 (2002).
[2] J. Clarke, Science **299**, 1850 (2003).
[3] G. Blatter, Nature **421**, 796 (2003).
[4] Y. Nakamura, Y. A. Pashkin, and J. S. Tsai, Nature **398**, 786 (1999).
[5] D. Vion et al., Science **296**, 886 (2002).
[6] Y. Yu et al., Science **296**, 889 (2002).
[7] S. Han et al., Science **293**, 1457 (2001).
[8] J. M. Martinis et al., Phys. Rev. Lett. **89**, 117901 (2002).
[9] J. R. Friedman et al., Nature **406**, 43 (2000).
[10] C. H. van der Wal et al., Science **290**, 773 (2000).
[11] I. Chiorescu et al., Science **299**, 1869 (2003).
[12] Y. A. Pashkin et al., Nature **421**, 823 (2003).
[13] T. Yamamoto et al., Nature **425**, 941 (2003).
[14] A. J. Berkley et al., Science **300**, 1548 (2003).
[15] R. McDermott et al., Science **307**, 1299 (2005).
[16] M. A. Nielsen and I. L. Chuang, *Quantum Computation and Quantum Information* (Cambridge University Press, Cambridge, 2000).
[17] A. Barenco et al., Phys. Rev. A **52**, 3457 (1995).
[18] B. L. T. Plourde et al., Phys. Rev. B **70**, 140501 (R) (2004).
[19] D. V. Averin and C. Bruder, Phys. Rev. Lett. **91**, 057003 (2003).
[20] A. Blais, A. M. van den Brink, and A. M. Zagoskin, Phys. Rev. Lett. **90**, 127901 (2003).
[21] X. Zhou et al., Phys. Rev. Lett. **89**, 197903 (2002).
[22] S. C. Benjamin, Phys. Rev. Lett. **88**, 017904 (2002).
[23] S. C. Benjamin and S. Bose, Phys. Rev. Lett. **90**, 247901 (2003).
[24] Z. Zhou, S.-I. Chu, and S. Han, IEEE Trans. Appl. Supercon. (2005, in press).
[25] V. V. Danilov, K. Likharev, and A. B. Zorin, IEEE Trans. Magn. **19**, 572 (1983).
[26] J. E. Mooij et al., Science **285**, 1036 (1999).
[27] S.-I. Chu, Chem. Phys. Lett. **167**, 155 (1990).
[28] M. R. Hermann and J. A. Fleck, Jr., Phys. Rev. A **38**, 6000 (1988).
[29] Z. Zhou, S. I. Chu, and S. Han, Phys. Rev. Lett. (submitted).